

Switchable Explosives: Performance Tuning of Fluid-Activated High Explosive Architectures

Cameron B. Brown^{1,2}, Alexander H. Mueller^{1,*}, Seetharaman Sridhar^{2,3}, Joseph P. Lichthardt¹,

Andrew M. Schmalzer¹, Bryce C. Tappan¹, Von H. Whitley⁴, Larry G. Hill¹,

Eduardo Lozano⁵ and Tariq D. Aslam⁵

¹*Q-5, High Explosive Science and Technology, Los Alamos National Laboratory, Los Alamos, New Mexico 87545, USA*

²*Colorado School of Mines, Golden, Colorado 80401, USA*

³*Arizona State University, Tempe, Arizona 85287-7805, USA*

⁴*XTD-SS, Safety and Surety, Los Alamos National Laboratory, Los Alamos, New Mexico 87545, USA*

⁵*T-1, Physics and Chemistry of Materials, Los Alamos National Laboratory, Los Alamos, New Mexico 87545, USA*

 (Received 21 September 2022; revised 17 January 2023; accepted 2 February 2023; published 17 March 2023)

We present our discovery of switchable high explosives (HEs) as a new class of energetic material that cannot detonate unless filled with a fluid. The performance of fluid-filled additive-manufactured HE lattices is herein evaluated by analysis of detonation velocity and Gurney energy. The Gurney energy of the unfilled lattice was 98% lower than that of the equivalent water-filled lattice and changing the fluid mechanical properties allowed tuning of the Gurney energy and detonation velocity by 8.5% and 13.4%, respectively. These results provide, for the first time since the development of HEs, a method to completely remove the hazard of unplanned detonations during storage and transport.

DOI: [10.1103/PhysRevLett.130.116105](https://doi.org/10.1103/PhysRevLett.130.116105)

Introduction.—Even with continued developments to create safer high explosives (HEs), accidents persist; a small arms survey documented more than 500 unplanned explosions at munitions sites between 1979 and 2013 [1]. The two-part binary HE, ammonium nitrate (AN) + fuel oil, is substantially less sensitive than other commercial blasting agents, but pure AN was still the primary HE responsible for the 2015 Tianjin and 2020 Beirut disasters that resulted in 369 combined fatalities [2,3]. The “holy grail” of a HE that is completely insensitive to unplanned stimuli but that switches to high performance during use is indisputably necessary but has not yet been realized, until now.

In contrast to insensitive explosives like AN that still detonates if a strong enough stimulus is applied to a large quantity of material, we present our discovery of “switchable” charges as HEs that can only be detonated after being filled with a mechanically activating fluid [4]. The ability of the HE structures in this work to switch on and off may be attributed to critical diameter effects [5,6]. A HE charge below the material critical diameter will not detonate in air because of energy losses from Prandtl-Meyer expansion fans formed at the HE-air interface. The expansion fans quench reactions near the HE surface so less energy is released in the detonation driving zone

bound by the detonation wave and the sonic locus. A stronger confinement material increases the pressure of shocks communicated between strands and mitigates the formation of Prandtl-Meyer expansion fans which enables an array of HE strands to sustain detonation below the critical diameter at which they fail when surrounded by air. Confinement effects in AM HE arrays are shown in Fig. 1.

In this Letter, we utilize additive-manufacturing (AM) methods to fabricate HE lattices composed of the 73 wt.% octahydro-1, 3, 5, 7-tetranitro-1, 3, 5, 7-tetrazocine (HMX)-based AMX 7301 ink formulation described in [4]. We quantify, for the first time, the detonative performance of switchable HE lattices by determination of the kinetic energy of expanding HE products and liner plates propelled by the HE (the Gurney energy). We are able to

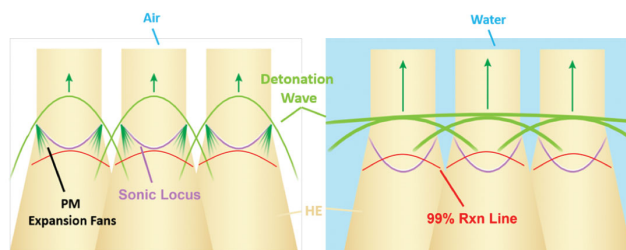


FIG. 1. Detonative switching effects in HE lattices. The HE lattices in this research cannot sustain detonation in air but can detonate when surrounded by a stronger confining fluid such as water. Water mitigates the formation of pressure expansion fans near the HE surface and it allows for the communication of stronger shock waves between adjacent HE strands.

Published by the American Physical Society under the terms of the [Creative Commons Attribution 4.0 International license](https://creativecommons.org/licenses/by/4.0/). Further distribution of this work must maintain attribution to the author(s) and the published article's title, journal citation, and DOI.

experimentally quantify switchability of the HE lattices and we are able to further tune the detonative performance by changing the mechanical properties of the fill fluids. The risk of unplanned detonations will be eliminated in applications utilizing switchable HE charges since the unfilled charges can be safely transported, handled, and stored without risk of detonation.

Materials and methods.—Experimental setup: Eight HE lattices were printed with 580 μm nozzles, 320 μm inter-strand spacing, 400 μm layer height, and 55.820 g nominal mass. Details of the AM system used in this research are described in the Supplemental Material [7]. An additional AMX 7301 charge was cast and tested as a control shot. The cast charge was pressed into a mold and cured at room temperature for 24 h under 20 psig N_2 . The cast charge mass was 75.457 g and the density was 1.693 g/cm^3 as measured using a lab scale and micrometers. The lattice structure and surface scan of a printed sample are shown in Fig. 3(a). Samples were sandwiched between two aluminum 6061 flyer plates with dimensions 80 mm \times 50 mm \times 4.7 mm and on the edges by two clear 3 mm thick PMMA windows. Two photon doppler velocimetry (PDV) probes were mounted on each side of the samples orthogonal to the plates to record flyer velocity for determination of the Gurney energy as shown in Fig. 2. The local charge mass C was determined via calculation of the HE volume fraction and fluid volume fraction at the PDV spot locations. Remington 44 AWG resin-coated copper magnet wires were fixed to a copper grounding strip on the interior surface of the rear acrylic window as detonation front time-of-arrival “makewire” diagnostics. The insulating resin coating on the wires prevented the circuits from closing even when the wires were energized with a +60 V potential as described in [8]. The lead shock in the detonation wave ionized the resin coating which shorted the individual makewire circuits. The detonation velocities were then calculated from the makewire positions on the samples and the detonation front arrival times.

Linewave generators were used to ensure the detonation wave breakout into samples was uniform [9]. The linewave generators were constructed using two layers of 4 mm

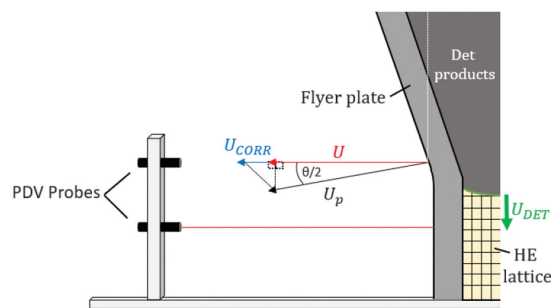


FIG. 2. Schematic of the experimental setup. Tilt corrections are applied to the measured PDV probe velocities to determine the flyer plate phase velocity resolved in the probe direction.

Primasheet P1000 as the slow detonating component and two layers of 4 mm Primasheet P2000 as the fast detonating component as shown in Fig. 3(b). Aluminized HE flash charges were used to illuminate the samples for high-speed imaging. Both the aluminized HE flash charges and the linewave generators were initiated with RP-80 detonators. The experimental setup is shown in Figs. 2, 3(c), and 3(d).

Various fill fluids were prepared to analyze the effects of fluid mechanical properties on HE detonation. Fluid densities and sound speeds were measured at 25°C using an Anton Paar DSA 5000 M density and sound velocity meter. Sample data and fill fluid properties are compiled in Table I.

A Specialized Imaging SIMX16 framing camera was used to image shots 2-4 and a Shimadzu HPV-X2 camera was used to image shots 1 and 5-9. The video was used as a secondary method of recording detonation velocity. Details of the fireset, instrumentation, and high-speed camera setup are described in the Supplemental Material [7].

Gurney energy: Detonation behavior of fluid-filled HE lattices in this work is assessed by analysis of the detonation velocity and the Gurney energy. Gurney energy measures the sum of the kinetic energy of expanding detonation products and liner plates driven by an explosive [10,11]. If a

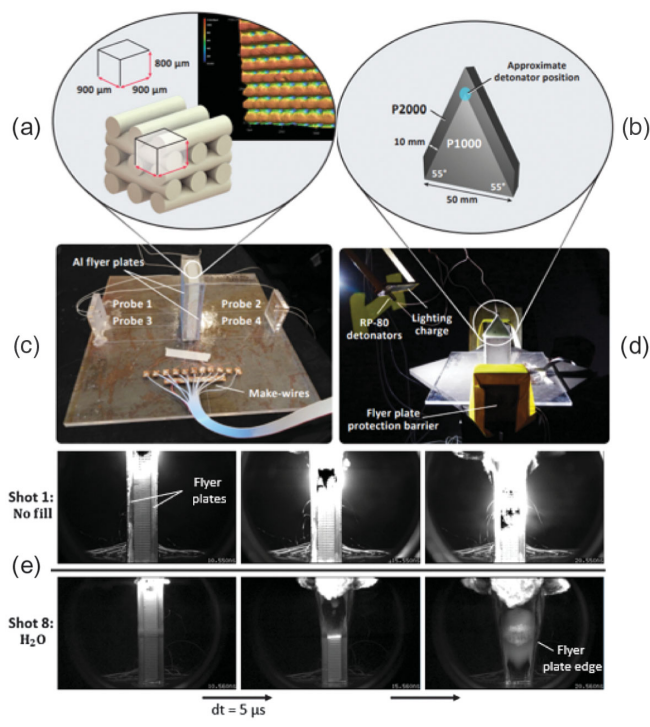


FIG. 3. Experimental setup and detonation time lapse. (a) Computer-generated model of AM HE structure and surface scan of a printed lattice. (b) Dimensions of the P1000/P2000 line wave generators. (c) Assembled shot with flyer plates, PDV probes, and makewires. (d) Assembled shot in blast vessel. (e) Time lapse of shots 1 and 8. Frames are shown at 5 μs intervals.

TABLE I. Sample and fill fluid data. Symbols are as follows: HE volume fraction at the PDV spot location (V_{fHE}), fluid density (ρ_f), fluid sound speed (c_f). Sodium Polytungstate is abbreviated as SPT. A trace amount (< 0.1 wt.%) of Triton X-100 was added to each aqueous solution to improve wettability in the lattices.

Shot No.	V_{fHE}	Fill fluid	ρ_f [g/cm ³]	c_f [m/s]
1	0.709	Air (Unfilled)	0.001	354.02
2	0.744	SPT + DIH ₂ O	2.724	1394.59
3	0.747	SPT + DIH ₂ O	2.865	1410.53
4	0.756	SPT + DIH ₂ O	1.703	1355.05
5	0.747	SPT + DIH ₂ O	2.236	1357.92
6	0.726	NaCl + DIH ₂ O	1.196	1795.99
7	0.738	Mineral oil	0.876	1456.65
8	0.750	DIH ₂ O	0.998	1499.00
9	1.000	None (Cast)

HE lattice failed to sustain detonation, the Gurney energy of the charge would be low because much of the chemical energy in the HE was not converted to kinetic energy to drive the liner plates. Gurney energy can also quantify changes in detonative performance due to the mechanical effects of fill fluids.

The equation for calculating the Gurney energy normalized per unit mass HE + fluid (E_{hf}) from a symmetrical sandwich shot configuration is given in Eq. (1),

$$\frac{U}{\sqrt{2E_{hf}}} = \left(\frac{M}{C} + \frac{1}{3}\right)^{-\frac{1}{2}}, \quad (1)$$

wherein U is the measured flyer velocity from the diffuse reflection off the plate surface, M is the sum of masses of the two flyer plates, C is the charge and fill fluid mass, and $1/3$ is a constant related to the specific symmetrical geometric configuration.

The Gurney Eq. (1) assumes that a fraction of the chemical energy stored in the HE is converted to kinetic energy as the detonation products expand along the $P - V$ isentrope [12,13]. Kennedy estimates that roughly 30% of the product energy is still present as the pressure drops to 1 kbar, but the majority of that energy cannot be transferred to the flyer plate because the system can only do work on the flyer plates during the adiabatic expansion process. Kennedy reported experimental efficiencies of 0.72–0.76 for Comp. B explosive and 0.61–0.65 for Trinitrotoluene [13]. The heat of detonation of the AMX 7301 HE used in this work was calculated by CHEETAH 9.0 thermochemical code to be 5.21 kJ/g. In the symmetrical sandwich configuration [14] a HE charge is sandwiched between two flyer plates and the detonation wave travels parallel to the plates [15,16]. Since the detonation velocity of HEs is on the order of km/s the energy transfer from the explosive to the liner plates is rapid; the detonation wave propagated through charges in this work in close to 10 μ s and flyer plates reached terminal velocities within around 16 μ s of the initial detonation events.

As the detonation wave propagates through the HE charge the flyer plates are bent and projected outwards with particle velocity (U_p) direction defined by the Taylor angle ($\theta/2$). For PDV probes mounted normal to the undisturbed flyer surface, the flyer plate phase velocity resolved in the probe direction is U_{CORR} . A schematic of the experimental setup and velocity vectors is shown in Fig. 2.

For the special case where PDV probes are mounted normal to the undisturbed plate surface, U_{CORR} can be calculated from the Taylor angle approximation using only U and the detonation velocity, U_{DET} . The corrected flyer velocity is determined by combining Eqs. (A1) and (A2) into the resultant Eq. (2) [17],

$$U_{CORR} = \frac{U}{\sqrt{1 - \frac{U^2}{U_{DET}^2}}}. \quad (2)$$

Equations (1) and (2) can then be rearranged to solve for E_{hf} as shown in Eq. (3),

$$E_{hf} = \frac{U_{CORR,ASY}^2}{2} \left(\frac{M}{C} + \frac{1}{3}\right), \quad (3)$$

wherein $U_{CORR,ASY}$ is the asymptotic corrected flyer velocity. Since the fill fluids used are assumed to be inert, the Gurney energy measured is imparted only by the HE mass and not the fluid mass so the total chemical energy released by the HE and by the HE + fluid system are the same. The specific energy normalized per unit mass of HE (E_h) [18] is therefore described by Eq. (4),

$$E_h = \frac{C}{m_{HE}} E_{hf}. \quad (4)$$

Results.—A time lapse of Shimadzu camera images for shots 1 and 8 is shown in Fig. 3(e). The time lapse shows that the H₂O-filled sample sustained detonation, whereas the unfilled sample does not. The unfilled sample instead deflagrates as evidenced by the saturated images and lack of a discernible detonation front. Lighter regions appeared in the fluid-filled H₂O and SPT–H₂O shots behind the detonation front which may indicate cavitation of bubbles trapped in the supercritical detonation product fluid [19,20]. Time lapse images of shots 5, 6, and 9 are included in the Supplemental Material as Fig. S1 [7].

The four PDV probe signals were combined into one averaged signal at each timestep and the combined velocity trace was adjusted via Eq. (2). The asymptotic flyer velocity ($U_{CORR,ASY}$) was calculated from the average value of the velocity trace over the last 2 μ s before flyer plate breakup. The sample standard deviation of the PDV measurements was calculated from the four PDV probe signals relative to $U_{CORR,ASY}$ over the last 2 μ s before plate breakup. The PDV data and statistical results are compiled in Table II and the adjusted flyer velocity traces are shown in Fig. 4(a).

TABLE II. Detonation velocity and Gurney energy results. No detonation velocity data are included for shot 2 since it failed to sustain detonation.

Shot No.	U_{DET} [km/s]	SE [km/s]	E_h [kJ/g]	1σ [kJ/g]
1	0.07	0.03
2	6.91	0.04	3.24	0.06
3	7.05	0.05	3.32	0.02
4	7.12	0.02	3.44	0.06
5	7.15	0.01	3.42	0.07
6	7.37	0.01	3.40	0.04
7	7.88	0.01	3.18	0.02
8	7.98	0.03	3.17	0.03
9	8.02	0.10	3.63	0.14

The initial high slope region of the flyer velocity traces is attributed to the oscillatory tensile and compressive motion of the plate due to shock wave reflections at the HE-air interfaces. Detonation velocity was calculated via makewires or camera data. If both camera and makewire data were collected for a shot, the time-of-arrival diagnostic that produced the lowest standard error in detonation velocity was used, and the associated statistical results are compiled in Table II. The detonation velocities of the fluid-filled shots are shown as a function of fluid density in Fig. 4(b). No detonation velocity was calculated for the unfilled sample because no makewire data were collected and the camera images were saturated. However, the saturated images indicated detonation failure which suggests a null detonation velocity.

The Gurney energy results are plotted as a function of fill fluid density in Fig. 5. Although they are not shown in the plot, the Gurney energies of the unfilled shot 1 and the cast shot 9 are 0.07 and 3.63 kJ/g, respectively, and are listed in Table II.

Discussion.—The detonative performance of a HE is influenced by the mechanical properties of the surrounding confining material. A stronger confiner mitigates pressure losses near the HE surface as the shock wave encounters the HE-confiner interface. An unconfined charge has a sonic locus that intersects the detonation front on the surface of the charge. Short’s model results quantified how stronger confining materials mitigated the formation of Prandtl-Meyer expansion fans as the shock moved across the HE-confiner interface, which shifted the sonic locus at the HE-confiner interface further downstream of the detonation front [21]. This shift allowed more chemical energy to be released in the subsonic detonation driving zone to better support the detonation front and increase the detonation velocity.

In this Letter, detonation velocity strongly decreased with increasing solution density as shown in Fig. 4(b). Since the detonation velocity should increase with confinement strength for HE near its critical diameter [22], the trend suggests that the 580 μm strands are below the material

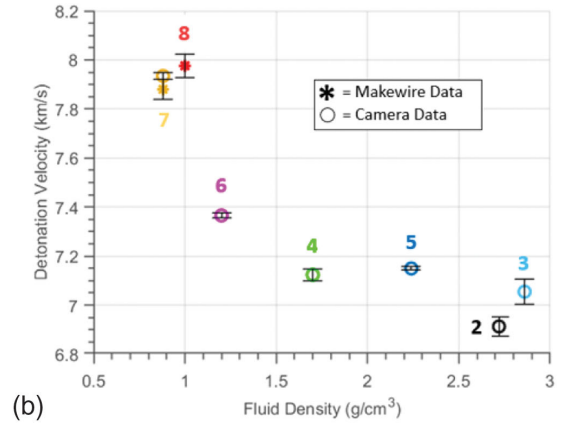
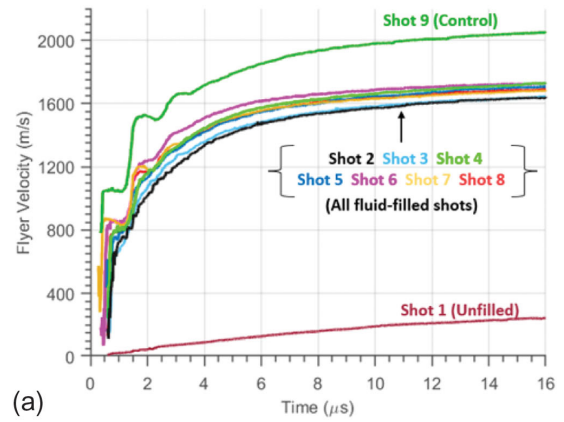


FIG. 4. (a) Flyer velocity traces. (b) Detonation velocities of fluid-filled shots. The 68% confidence interval bounds are shown. Makewire data were only available for shots 7 and 8.

critical diameter for the fluids used in this research and that the filled lattices were behaving more as a homogeneously detonating charge than independently-functioning 580 μm strands. Figure 5 shows that the Gurney energy normalized per unit mass HE + fluid (E_{hf}) decreases with fluid density

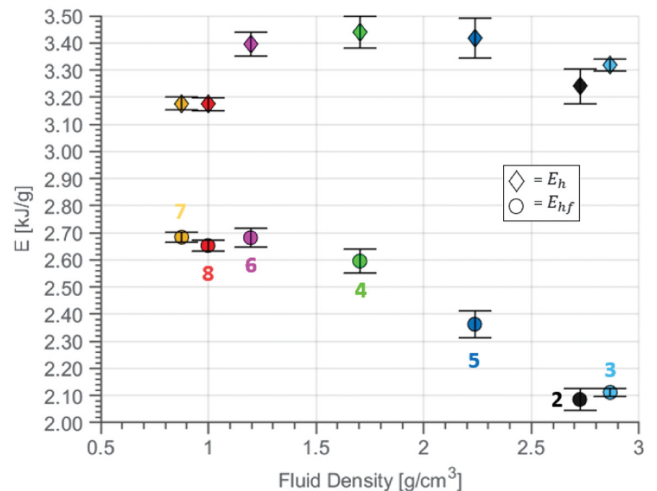


FIG. 5. Gurney energy results for the fluid-filled shots are shown with 68% confidence interval bounds.

and that the Gurney energy normalized per unit mass HE (E_h) shows a somewhat cubic behavior with increasing fluid density.

The experimental Gurney energies for the fluid-filled and cast charge are reasonable compared to other commonly used explosives; Kennedy reports that Comp-B explosive has a Gurney energy of 3.64 kJ/g and PBX 9404 has a Gurney energy of 4.22 kJ/g [13,23]. The reduction in E_h for the cast charge compared to the predicted heat of detonation value of 5.21 kJ/g is expected because of the thermodynamic and mechanical losses. The experimental cast charge efficiency of 69.7% is within the bounds of expected efficiencies as compared to Kennedy's results [13].

PDV results verified that the unfilled lattice failed to sustain detonation since its E_h was 98% lower than that of an equivalent water-filled structure. The results also indicated that the mechanical properties of the fill fluid influence the Gurney energy. The E_h for shot 4 increased 8.5% relative to the water-filled shot, but E_h then decreased for higher density fill fluids. Overlap in 2σ error bounds prohibits the interpretation of the Gurney energy results for shots with fluid density higher than 2.24g/cm³ in relation to the lower fluid density shots 7 and 8. However, confidence in the Gurney energy results for the higher fluid density shots 4, 5, and 6 relative to the lower fluid density shots 7 and 8 is high because the 2σ error bounds of the lower density and higher density fill fluid shots do not overlap.

The switchable lattices may function in both the homogeneous and heterogeneous detonation regimes as described by Lee *et al.* and Frost *et al.* [24–26]. If the diameter of HE confined by fluid in the channels is above the critical diameter, strands of HE would detonate independently of each other in the heterogeneous detonation regime. If the diameter of HE confined by fluid in the channels is below the critical diameter, strands would detonate by the coalescence of detonation waves through the surrounding fluid in the homogeneous sympathetic detonation regime. An increase in the density of the fluid confining the subcritical diameter strands may increase the shock impedance, but the detonation velocity would be expected to decrease because energy in the reaction zone is transferred to kinetic energy to accelerate the fluid diluent particles since the HE and fill fluid behave homogeneously [27–29]. In this Letter, the increase in Gurney energy with increasing fluid density indicates some amount of heterogeneous behavior, but the decrease in detonation velocity with increasing fluid density is indicative of homogeneous detonation behavior. Therefore, the regimes are inherently coupled in the fluid-filled HE lattices, and optimization of the Gurney energy requires a robust understanding of how fluid properties affect detonation in the different regimes.

Conclusion.—This research demonstrated that the energy output of unfilled AM HE lattice structures is 98% less than that of an equivalent water-filled structure, so the unfilled HE lattice may only deflagrate and does not pose a

detonation risk. The detonative performance can further be tuned for specific applications by the fill fluid; higher density fluids increase E_h by up to 8.5% and decreased detonation velocity by 13.4% relative to the water-filled shot. A quantitative understanding of the mechanical effects of fluids as confiners and shock transmission media is needed to tune detonative performance in the switchable lattices. The data presented in this Letter only apply to a narrow range of HE structure lattice parameters and volume fractions; Gurney energy data for any new structures with different lattice parameters and HE strand diameters are needed to understand how the structures behave and to ensure they can be safely switched on when in use but remain insensitive during storage, transport, and handling.

All experimental data produced in this research will be made available upon request. However, the exact details of the HE formulation used are controlled.

Thanks to E. Francois for assistance with the experimental setup, E. S. Davis and P. Vakhlamov for fluid properties measurements, D. Judge for help with illustration visual design, and V. Manner for editing assistance. We would also like to thank Jason Loiseau of the Royal Military College of Canada for helpful discussions in the setup of flyer plate experiments. This work was supported by the U.S. Department of Energy through the Los Alamos National Laboratory. Los Alamos National Laboratory is operated by Triad National Security, LLC, for the National Nuclear Security Administration of U.S. Department of Energy (Contract No. 89233218CNA000001). Research presented in this paper was supported by the Laboratory Directed Research and Development program of Los Alamos National Laboratory under Projects No. 20200463MFR, No. 20160103DR, and No. 20200623ER. The switchable explosive effect was discovered through projects funded by LANL's Laboratory Directed Research and Development program. Characterization of the performance differences (Gurney energy and detonation velocity) was supported by the Los Alamos National Laboratories office of experimental science Dynamic Material Properties campaign. Authors declare that they have no competing interests.

*Corresponding author.
amueller@lanl.gov

- [1] E. Berman and P. Reina, Unplanned Explosions at Munitions Sites (UEMS): Excess Stockpiles as Liabilities rather than Assets, *Small Arms Surv.* (2014).
- [2] J.-J. Zhang, T.-B. Wang, D. Fan, J. Zhang, and B. Jiang, Medical response to the tianjin explosions: Lessons learned, *Disaster Med. Public Health Prep.* **12**, 411 (2017).
- [3] M. S. Hajjar, G. M. Atallah, H. Faysal, B. Atiyeh, J. Bakhach, and A. Ibrahim, The 2020 Beirut explosion: A healthcare perspective, *Ann. Burns Fire Disasters* **34** (2021).

- [4] A. Schmalzer, A. Mueller, B. Tappan, V. Whitley, P. Bowden, and Z. Roberts, Advanced manufacturing applications at Los Alamos National Laboratory, *JDR&E* **3**, 81 (2020).
- [5] C. M. Tarver and E. M. Mcguire, Reactive flow modeling of the interaction of tatb detonation waves with inert materials. Lawrence Livermore national laboratory (2002), <http://www.intdetsymp.org/detsymp2002/PaperSubmit/FinalManuscript/pdf/Tarver-069.pdf>.
- [6] T. Aslam, J. Bdzil, and L. Hill, Analysis of the LANL detonation-confinement sandwich test, Technical Report, Los Alamos National Laboratory, 2003.
- [7] See Supplemental Material at <http://link.aps.org/supplemental/10.1103/PhysRevLett.130.116105> for further experimental detail, derivation of tilt correction equations, and additional high-speed video images.
- [8] B. Tappan, P. Bowden, J. Lichthardt, M. Schmitt, and L. Hill, Evaluation of the detonation performance of insensitive explosive formulations based on 3, 3' Diamino-4, 4'-Azoxyfurazan (DAAF) and 3-Nitro-1,2,4-Triazol-5-One (NTO), *J. Energetic Mater.* **36**, 169 (2018).
- [9] J. Morris, S. Jackson, and L. Hill, A simple line wave generator using commercial explosives, *AIP Conf. Proc.* **1195**, 408 (2009).
- [10] R. W. Gurney, Aberdeen Proving Ground, USA (1943).
- [11] J. Dehn, U.S. Army Ballistic Research Laboratory (1984).
- [12] W. Davis and W. Fickett, *Detonation: Theory and Experiment* (Dover Publications, New York, 1979).
- [13] J. Kennedy, Gurney energy of explosives: Estimation of the velocity and impulse imparted to driven metal, Technical Report, Sandia Laboratories, 1970.
- [14] L. Hill, Development of the LANL sandwich test, Technical Report, Los Alamos National Laboratory, 2001.
- [15] J. Loiseau, W. Georges, D. Frost, and A. Higgins, *Shock Waves* **709** (2018).
- [16] J. Loiseau, O. E. Petel, J. Huneault, M. Serge, D. Frost, and A. J. Higgins, Acceleration of plates using non-conventional explosives heavily-loaded with inert materials, *J. Phys. Conf. Ser.* **500**, 182027 (2014).
- [17] L. Hill, in 19th Biennial APS Conference on Shock Compression of Condensed Matter (SCCM15), *Proceedings of the AIP Conference* (2015).
- [18] C. Rumchik, An investigation on the effect of aluminum particle size on detonation, metal acceleration, and airblast, Ph.D. thesis, University of Minnesota, 2015.
- [19] W. Wu, Y. Liu, A. Zhang, N. Liu, and L. Liu, Numerical investigation on underwater explosion cavitation characteristics near water wave, *Ocean Eng.* **205**, 107321 (2020).
- [20] A. Milne, A. Longbottom, D. Frost, J. Loiseau, S. Goroshin, and O. Petel, Explosive fragmentation of liquids in spherical geometry, *Shock Waves* **27**, 383 (2017).
- [21] M. Short and J. Quirk, High explosive detonation–confiner interactions, *Annu. Rev. Fluid Mech.* **50**, 215 (2018).
- [22] C. Souers, P. Vitello, S. Esen, J. Kruttschnitt, and H. Bilgin, The effects of containment on detonation velocity, *Propellant Explos. Pyrotech.* **29**, 19 (2004).
- [23] J. Zukas, W. Walters, and W. Walters, *Explosive Effects and Applications*, High pressure shock compression of condensed matter (Springer, New York, 2002).
- [24] J. Lee, D. Frost, and J. Lee, *Shock Waves* **115** (1995).
- [25] J. Lee, Detonation mechanisms in a condensed-phase porous explosive, Ph.D. thesis, University of Sherbrooke, Quebec, Canada, 1997.
- [26] D. Frost, T. Aslam, and L. Hill, Application of detonation shock dynamics to the propagation of a detonation in nitromethane in a packed inert particle bed, *AIP Conf. Proc.* **505**, 821 (2000).
- [27] W. Wilson, The influence of inert particulate material on the properties of RDX/polyethylene wax compositions, Technical Report, Department of defense materials research laboratories, Report No. MRL-9-929, 1984.
- [28] M. A. Cook, Compressibilities of solids and the influence of inert additives on detonation velocity in solid explosives, *Discuss. Faraday Soc.* **22**, 203 (1956).
- [29] I. Voskoboinikov and A. Kotomin, *Combust. Explos. Shock Waves* **200** (1985).